# Micropipette Aspiration on the Outer Hair Cell Lateral Wall

P. Sidney Sit,* Alexander A. Spector,* Allen J-C. Lue,# Aleksander S. Popel,* and William E. Brownell#
*Department of Biomedical Engineering, The Johns Hopkins University, Baltimore, Maryland 21205, and #Bobby R. Alford Department of Otorhinolaryngology and Communicative Sciences, Baylor College of Medicine, Houston, Texas 77030 USA

ABSTRACT The mechanical properties of the lateral wall of the guinea pig cochlear outer hair cell were studied using the micropipette aspiration technique. A fire-polished micropipette with an inner diameter of ~4 $\mu$m was brought into contact with the lateral wall and negative pressure was applied. The resulting deformation of the lateral wall was recorded on videotape and subjected to morphometric analysis. The relation between the length of the aspirated portion of the cell and aspiration pressure is characterized by the stiffness parameter, $K_s$ = 1.07 ± 0.24 (SD) dyn/cm ($n$ = 14). Values of $K_s$ do not correlate with the original cell length, which ranges from 29 to 74 $\mu$m. Theoretical analysis based on elastic shell theory applied to the experimental data yields an estimate of the effective elastic shear modulus, $\mu$ = 15.4 ± 3.3 dyn/cm. These data were obtained at subcritical aspiration pressures, typically less than 10 cm $H_2O$. After reaching a critical (vesiculation) pressure, the cytoplasmic membrane appeared to separate from the underlying structures, a vesicle with a length of 10–20 $\mu$m was formed, and the cytoplasmic membrane resealed. This vesiculation process was repeated until a cell-specific limit was reached and no more vesicles were formed. Over 20 vesicles were formed from the longest cells in the experiment.

## INTRODUCTION

Mammalian hearing begins with the mechanical displacement of sensory cells in the organ of Corti. The organ of Corti is located on the basilar membrane and, together with the tectorial membrane, makes up the cochlear partition. Acoustic signals are separated spectrally as a result of passive and active mechanical filtering in the cochlea. Passive mechanical filtering is engendered by the elastic, viscous, and inertial properties of the structures that make up the cochlear partition and its surrounding fluids. The passive filtering is enhanced by an active process that adds mechanical energy and further narrows the bandpass filtering occurring at a given location along the length of the cochlear partition. It is currently thought that electrically evoked length changes (known as electromotility) of the outer hair cell (OHC) provide the mechanical energy for this active feedback. We have examined the mechanical properties of the outer hair cell to better evaluate the cell's contribution to both passive and active filtering. Specifically, we apply the micropipette aspiration technique to measure the elastic properties of the OHC lateral wall. This technique also permits a characterization of the forces of association between the components of the lateral wall.

### Structural features of the outer hair cell

The outer hair cell is an epithelial cell with a cylindrical shape that resides in a highly organized cellular matrix. It contacts other cells only at its apical and basal poles. Its lateral walls are separated from nearby cells by the large fluid-filled spaces of Nuel. The OHC is divided into three functional regions—apical pole, basal pole, and lateral wall—with separate structural features. The mechanoelectrical transduction characteristic of all hair cells is associated with the stereocilia bundle at the cell's apical pole. Electrochemical transduction occurs at synaptic structures at the cell's basal pole. The electromechanical transduction responsible for outer hair cell electromotility is associated with the cell's lateral wall. The lateral wall is a trilaminate structure consisting of the cytoplasmic membrane, a cortical lattice, and a subsurface cisternal system. All three layers are found within 100 nm of the cell's outer surface.

Electron microscopy reveals structural differences in the OHC cytoplasmic membrane among the three structural/functional regions of the cell. The cytoplasmic membrane is the outermost layer of the lateral wall, and in transmission electron micrographs it is partially folded. This rippling makes it difficult to achieve a transverse section through long portions of the membrane, and as a result the cytoplasmic membrane of the lateral wall appears almost translucent. Its appearance contrasts with the cytoplasmic membranes at the OHC's apical and basal end, which are not folded and appear as distinct crisp bilayers (Brownell, 1990).

The tenuous appearance of the lateral wall cytoplasmic membrane also contrasts with the crisp membranes that make up the subsurface cisterna (SSC). The SSC is a subcellular organelle that forms the innermost layer of the lateral wall. It is composed of concentric layers of agranular flattened membranes (Saito, 1983; Evans, 1990; Dieler et al., 1991; Slepecky and Ligotti, 1992). In outer hair cells

*Received for publication 1 August 1996 and in final form 16 March 1997.*
Address reprint requests to Dr. William E. Brownell, Bobby R. Alford Department of Otorhinolaryngology and Communicative Sciences, Baylor College of Medicine, Houston, TX 77030. Tel.: 713-798-8540; Fax: 713-798-8553; E-mail: brownell@bcm.tmc.edu.

Dr. Sit's present address is Department of Physiology and Biophysics, School of Medicine, Case Western Reserve University, Cleveland, OH 44106.

0006-3495/97/06/2812/08 $2.00

isolated from the guinea pig cochlea, there is an almost unbroken single cisterna that extends from the basal synaptic region to the tight junctional complexes at the cell's apical end. This cylindrically concentric compartment is composed of an inner cisternal membrane and an outer cisternal membrane separated by 20–30 nm. The content of the intracisternal space is unknown. The SSC divides the cell into an axial core and an extracisternal space. Cisternal stacks are also present over ~20% of the lateral wall (Dieler et al., 1991) with a structural similarity to the Golgi apparatus or endoplasmic reticulum (ER). The SSC may be labeled by lipid-specific markers for both Golgi and ER (Pollice and Brownell, 1993), suggesting that the SSC shares properties of both.

The extracisternal space is created by the outer cisternal membrane and the cytoplasmic membrane, which are separated by a varying distance of ~40 nm. The ripples in the cytoplasmic membrane give rise to a variation of ±20 nm. Lying adjacent to the outer cisternal membrane is a cytoskeletal network called the cortical lattice (Bannister et al., 1988; Holley and Ashmore, 1988, 1990a; Holley et al., 1992). The two-dimensional cortical lattice has been shown to consist of actin filaments and spectrin cross-links (Flock et al., 1986; Holley and Ashmore, 1990b). Pillars extend from the cortical lattice to the folded cytoplasmic membrane (Flock et al., 1986; Bannister et al., 1988; Arima et al., 1991; Holley et al., 1992). The OHC is a cellular hydrostat (Brownell, 1990; Brownell and Shehata, 1990), and its shape is maintained by the tensile force of the filaments (Holley and Ashmore, 1990b), the SSC, and the positive hydrostatic pressure of the cytoplasm.

### Micropipette aspiration

Micropipette aspiration is one of the experimental methods used in the studies of mechanical properties of cells (Evans and Skalak, 1980; Hochmuth, 1990). It has been used extensively to study the membrane properties of erythrocytes (Evans, 1973; Chien et al., 1978; Evans and Kukan, 1984), polymorphonuclear leukocytes (Schmid-Schönbein et al., 1981; Evans and Kukan, 1984; Ruef et al., 1991), lymphocytes and monocytes (Ruef et al., 1991), platelets (Burris et al., 1986, 1987; Smith et al., 1989), bovine aortic endothelial cells (Sato et al., 1987a,b), and macrophages (Mege et al., 1987). This method allows accurate estimation of the parameters for describing regional variation of material properties.

We have examined the mechanical properties of the OHC lateral wall by measuring displacements produced in response to micropipette aspiration. We calculate the lateral wall stiffness and compare it with other cell types. Theoretical analysis based on elastic shell theory permits the calculation of an effective elastic shear modulus from the stiffness parameter. When larger suction pressures are used, the cytoplasmic membrane releases vesicles into the micropipette.

## MATERIALS AND METHODS

Pigmented guinea pigs (200–250 g, of either sex) were anesthetized by exposure to 100% $CO_2$ and decapitated by guillotine. The temporal bones were removed and OHCs were isolated using techniques that have been described elsewhere (Brownell et al., 1985; Pollice and Brownell, 1993; Chertoff and Brownell, 1993). The cells were harvested and maintained in a standard medium consisting of phosphate-buffered saline (PBS, Dulbecco's) supplemented with (in mM) 1.5 $CaCl_2$, 1.5 $MgCl_2$, and 10 D-glucose. Solutions had an osmolarity of 290–305 mOsm and a pH of 7.3–7.4, and were at room temperature (20–22°C). The experiments were conducted in a 2-mm deep, 2 × 5 cm rectangular recording chamber constructed on a glass coverslip. The chamber was filled with the standard solution and 0.5 mg/ml bovine serum albumin (BSA). Isolated cells were plated onto the chamber, which was then placed on the stage of a Zeiss IM-35 inverted microscope. All cells were observed with a 100× objective lens (Zeiss, N.A. 1.4) and monitored with video-enhanced contrast, using a Dage-MTI Newvicon camera and amplifier. Images were monitored and recorded (S-VHS format) for subsequent analysis. The time and date were superimposed and recorded on the video image.

Aspiration micropipettes were fabricated from a borosilicate glass capillary (Dagan LG16, 1.65 μm O.D.) using a programmable micropipette puller (BB-CH-PC; Mecanex, Geneva). The tip was broken, shaped, and fire-polished with a microforge (De Fonbrune, St. Louis, MO). The inner diameter of the micropipette tip was about 4 μm, with a shallow taper that could not be measured over the >10-μm length that was in the microscope's field of view (see Fig. 1). The micropipette was mounted on a joystick-controlled manipulator and advanced at a shallow angle (<20° to the stage) to the center of the field of view. The micropipette was connected to a water column via polyethylene tubing (Intramedic, no. 205). The entire fluid system was filled with the standard solution and 0.05 mg/ml BSA. The null point of the pressure scale was referenced to the level of the microscope stage and was the level at which no fluid movement occurred at the micropipette tip.

An isolated cell was selected for study based on standard morphological criteria under the light microscope. Healthy cells displayed a characteristic birefringence and a transparent cytoplasm in the axial core immediately

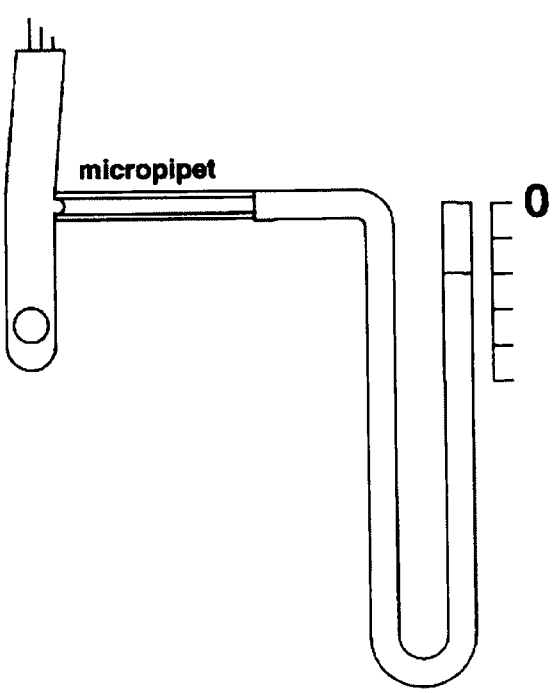


FIGURE 1 Schematic diagram showing micropipette aspiration experiment on OHC.

above an eccentrically placed nucleus, which was found near the synaptic pole. Cells were excluded if Brownian movement of cytoplasmic particles was present. Selected cells possessed cuticular plates with or without stereocilia. Experiments were carried out on 14 cells from five cochlea.

Once a cell was located, the microscope stage was rotated to orient the OHC's longitudinal axis at a right angle to the micropipette. The micropipette was then brought into contact with the OHC's lateral wall. Unless otherwise indicated, all results are based on the micropipette contacting the lateral wall at a point midway ($\pm 4$ $\mu$m) between the nucleus and the cuticular plate. Negative pressure was applied in 1-cm increments as measured from the null point. Single frames of video images were captured from the videotape by using a Synoptics framegrabber and software package (Semper, Synoptics). Digitized videomicrographs of the aspiration process were subjected to morphometric analysis. The protocol for whole cell tracing and calculating area, length, and width of each cell was described previously (Chertoff and Brownell, 1993). Tongue length was measured from the apex of the aspirated portion of the lateral wall inside the micropipette to the micropipette tip using a commercial software package (Comos; Bio-Rad). The astigmatism of the framegrabber was corrected digitally using a MATLAB program (Mathworks). The inner radius of the micropipette tip was corrected for the cylinder lens enlargement resulting from the difference in refractive indices of glass and the perfusion solution (Engström et al., 1992).

## Theoretical relationship between stiffness parameter and shear modulus

The stiffness parameter of the cell is used to characterize the elastic response of a cell to the application of the external load (see e.g. Sato et al., 1987a,b; Evans, 1973; Theret et al., 1988). The stiffness parameter is a function of elastic properties and the geometry of the cell. The derivation of this function is based on the solution of corresponding problems of theory of elasticity. Theret et al. (1988) and Cheng (1987) give examples of such analysis for an elastic half-space and an elastic sphere, considering the deformations of endothelial cells and sea urchin eggs under the conditions of the micropipette aspiration experiment.

The model of a three-dimensional elastic body involves all modes of the stress-strain state allowed by Hooke's Law and equilibrium conditions. Thin elastic structures may be modeled as membranes or shells. Each model is based on different assumptions concerning the internal stress-strain state of the wall. Membranes can sustain in-plane stretching and shearing, but do not resist out-of-plane bending and twisting. An elastic membrane is a common model of the cell wall (Evans and Skalak, 1980). A shell model of a thin structure includes bending and twisting modes of the stress-strain state as well as membrane modes.

The micropipette in our experiments is applied to an elongated cylindrical OHC, which results in local loading of the lateral wall. The membrane model of a thin wall is unable to deal with localized loads (Novozhilov, 1959). Because of this, our derivations of the relationship between the stiffness parameter and shear modulus are based on shell theory (Spector et al., 1996a).

After a linear analysis, we decompose the stress-strain state of the OHC wall into two parts. The first state occurs in the closed shell under the action of uniform internal pressure. The second one corresponds to the open cylindrical shell under the pipette action. We concentrate on the latter component, which determines the values measured in the micropipette experiment. We use the equations relating membrane forces, shear forces, and bending and twisting moments to elastic displacements governed by the Donnell-Mushtari-Vlasov version of shell theory (Calladine, 1983; Dym, 1990). A more detailed analysis based on exact shell equations (e.g., Niordsen, 1985; Novozhilov, 1959) shows that the Donnell-Mushtari-Vlasov version gives a good approximation of our problem (Spector et al., 1996a). The latter approach is simpler, and it allows us to obtain the final results in analytical form. The problem is reduced to a differential equation with respect to the radial component $w$ of the displacement. It takes the form

$$k\nabla^8 w + \frac{1-\nu^2}{R^4}\frac{\partial^4 w}{\partial x^4} = \frac{1}{R^2 D}\nabla^4 p \tag{1}$$

Here $k = B/Dr^2$ is the ratio of a characteristic of the bending resistance of the wall material to a characteristic of its stretching resistance, $B = Eh^3/(12(1-\nu^2))$, $D = Eh/(1-\nu^2)$, $R$ is the radius of the shell, $h$ is its thickness, $\nu$ is Poisson's ratio, and $E$ is Young's modulus. $\nabla^2$ is the Laplace operator with respect to $x$ and $\phi$, where $x$ is the direction along the cell, and $\phi$ is the circumferential direction (Fig. 2). We assume that $p = p(x, \phi)$ is equal to the aspiration pressure at the points inside the internal contour of the micropipette and to the normal reaction pressure at the points of the contact area of the micropipette edge and the cell surface. This reaction is determined by the force balance in the direction of the pipette axis.

We obtain the solution to Eq. 1 in terms of a Fourier series with respect to the circumferential coordinate. Using infinite cylinder approximation, we can find analytically the deformational response to every circumferential harmonic and, as a result, closed formulae for the Fourier coefficients. Based on a three-term representation of a series, we derive the following formula for the length of the aspirated tongue ($L_t$) in terms of the cell's membrane elastic properties and the geometry of the cell and pipette

$$L_t = \frac{\sqrt{2}p_p R R_i (1-\nu^2)^{0.75}}{2\pi\mu(1+\nu)\kappa^{0.75}} \frac{\alpha[\alpha f(\alpha_i) - f(\alpha_o)]}{\alpha^2 - 1} \tag{2}$$

where

$$f(x) = -0.33x^2 + 0.43x$$

$$\kappa = \frac{1}{12}\left(\frac{h}{R}\right)^2, \quad \alpha = \frac{R_o}{R_i}, \quad \alpha_i = \frac{R_i}{R}, \quad \alpha_o = \frac{R_o}{R}$$

Here $\mu$ is the shear modulus used in cell mechanics, $p_p$ is the magnitude of aspiration pressure, and $R_i$ and $R_o$ are the respective inner and outer radii of the pipette.

By using the common definition of the stiffness parameter $K_s$ in terms of the length of the aspirated tongue,

$$K_s = \frac{-p_p R_i^2}{L_t} \tag{3}$$

we obtain

$$K_s = \frac{\sqrt{2}\pi\mu(1+\nu)\kappa^{0.75} R_i}{(1-\nu^2)^{0.75} R} \frac{\alpha^2 - 1}{\alpha[\alpha f(\alpha_i) - f(\alpha_o)]} \tag{4}$$

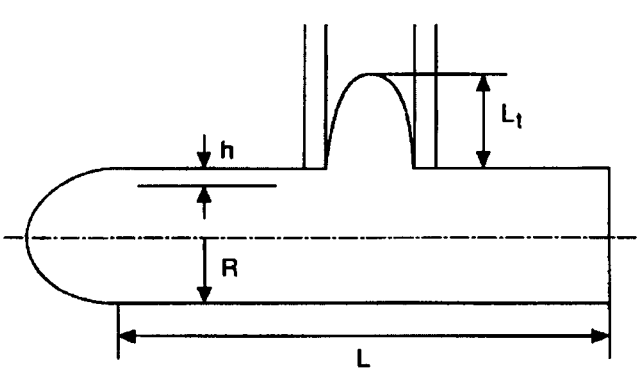


FIGURE 2 Drawing of OHC identifying geometric variables involved in the application of shell theory to the experiment.

When the outer radius of the pipette is greater then the radius of the cell (i.e., $R_0 > R$), the cell and the pipette surfaces are in contact over a part of the pipette bottom. In this case, we use a correction of formulae 2 and 4, replacing in them $R_o$ by $\frac{1}{2}(R_o + R)$.

## RESULTS

### Elastic properties of the lateral wall

Fig. 3 presents three digitized videomicrographs and Fig. 4 the corresponding schematic drawing showing the elastic deformation of the OHC's lateral wall when it is subjected to micropipette aspiration. Before the critical pressure (vesiculation pressure) is reached, the length of the portion of the lateral wall (tongue) aspirated into the micropipette increases with the magnitude of the negative pressure. A typical experiment lasts 5 min. At a pressure greater than $-2$ cm $H_2O$, a slight bending of the cell is observed. The cell bends about the place of attachment of the micropipette, and both the apical and the basal ends move toward the micropipette. In some experiments, hysteresis is observed, but we have not systematically investigated this phenomena.

The experimental results reveal a linear relationship between the aspirating pressure, $p_p$, and the tongue length, $L_t$:

$$-p_p R_i = K_s \frac{L_t}{R_i} + K_i \tag{5}$$

The slope of this relation, $K_s$, is the stiffness parameter. There is a nonzero intercept $K_i$ in the experimental data for some cells. The relationship between $-p_p R_i$ and $L_t/R_i$ for a sample set of eight cells from one cochlea is shown in Fig.

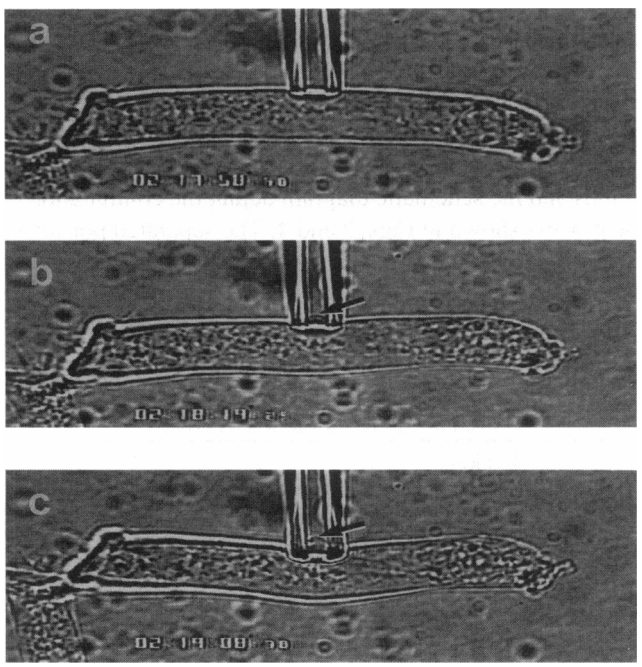


FIGURE 3 Three digitized videomicrographs showing different stages of the elastic deformation of an OHC lateral wall during micropipette aspiration. Cell length 78 $\mu$m; cell width 10 $\mu$m. (*a*) A typical cylindrical isolated outer hair cell. Date and time are recorded at the lower left-hand corner. The nucleus is located eccentrically at the cell's base, which is located on the right. Fragments of synaptic remnants are still attached to the base of the cell. (*b*) Elastic deformation of the lateral wall at $p_p = -6$ cm $H_2O$ after mechanical equilibrium is established. The leading edge of the tongue can be seen several microns above the micropipette tip (marked by an *arrow*). The cell bends slightly about the attachment point of the micropipette. (*c*) Elastic deformation at $p_p = -10$ cm $H_2O$. The cell bends in the direction of the micropipette.

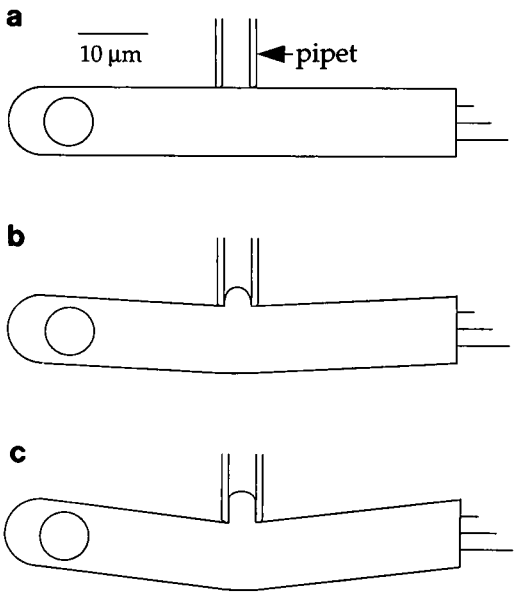


FIGURE 4 Schematic drawing of aspiration sequence shown in Fig. 1. (*a*) The micropipette is attached to the OHC cytoplasmic membrane. No negative pressure is applied, and the lateral wall is not deformed. (*b*) After a negative pressure below a critical value is applied, a portion of the lateral wall (tongue) is aspirated into the micropipette. The length of the tongue increases linearly with the magnitude of the applied pressure. (*c*) A higher negative pressure is applied and the tongue is longer. The cell is bent in the direction of the micropipette. If the negative pressure is released before a critical pressure for vesiculation is reached, the tongue retracts to the original position.

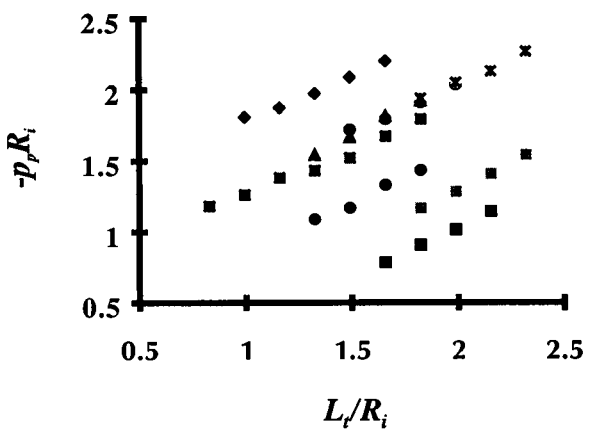


FIGURE 5 A typical plot of the elastic deformation as a function of applied negative pressure for eight different cells. $L_t$, length of the tongue; $R_i$, inner radius of the micropipette; $-p_p$, applied pressure.

5. The mean value of the stiffness parameter for this set of cells is 1.19 ± 0.12 dyn/cm.

The results of aspiration experiments with 11 different cells from five cochlea are shown in Table 1. The high values of the correlation coefficient, $r$, indicate that the relationship between aspirating pressure and tongue length is close to linear for each cell. The stiffness parameter is determined for each cell, and the mean value is $K_s$ = 1.07 ± 0.24 (SD) dyn/cm, $n$ = 14. The values of the stiffness parameter for individual cells are shown in Fig. 6 versus cell length. Statistical analysis of these data indicates that there is no significant correlation between stiffness parameter and the original cell length or cell radius (taken as half of the cell width).

Using Eq. 4, we can express the elastic shear modulus $\mu$ for the lateral wall in terms of the experimentally determined stiffness parameter ($K_s$), cell radius ($R$), lateral wall thickness ($h$), pipette inner ($R_i$) and outer ($R_o$) radii, and Poisson's ratio ($\nu$). Results of these calculations are presented in the right column in Table 1 for individual cells, with a mean value for the population of $\mu$ = 15.4 ± 3.3 (SD) dyn/cm. The inner pipette radius was measured for each pipette, and the same pipette was used for OHCs collected from the same cochlea ($R_i$ = 1.54 ± 0.04 (SD) μm, $n$ = 7). The thickness of pipette wall, $R_0 - R_i$, was 1.54 ± 0.04 (SD) μm, $n$ = 14. The thickness of the OHC lateral wall ($h$) was estimated as 100 nm based on electron micrographs (Dieler et al., 1991). Poisson's ratio $\nu$ is expressed in terms of the ratio of the shear modulus $\mu$ and area expansion modulus $K$ in the form $\nu = (1 - \mu/K)/(1 + \mu/K)$ (Spector et al., 1996a). The value $\mu/K$ = 0.054 (Ratnanather et al., 1996) and corresponding $\nu$ = 0.90 were used for the calculation of the shear modulus. The substitution of Poisson's ratio $\nu$ = 0.82 (Iwasa and Chadwick, 1992) leads to $\mu$ = 24.1 dyn/cm. The sensitivity of $\mu$ to differences in the lateral wall thickness may be estimated by allowing for variation in the value of $h$; we obtain $\mu$ = 23.6 ± 5.1 dyn/cm for $h$ = 75 nm and $\mu$ = 11.0 ± 2.4 dyn/cm for $h$ = 125 nm.

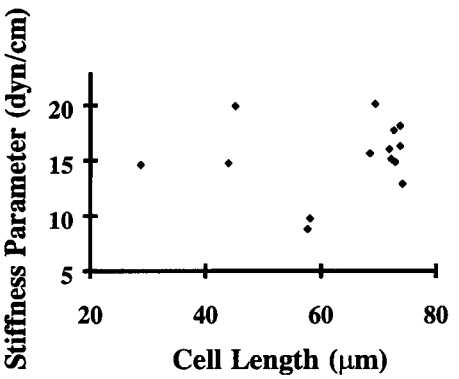


FIGURE 6 Stiffness parameters obtained in experiments with 14 OHCs from five cochleae plotted against the original length of the cells.

## Vesiculation of the lateral wall

Irreversible changes begin when a cell-specific critical aspiration pressure is reached (typically around −10 cm $H_2O$). This phenomenon is examined in a separate series of experiments. The aspiration pressure remains constant once the vesiculation pressure is reached. At this pressure the cytoplasmic membrane appears to separate from the underlying structures, and two distinct layers become visible inside the pipette (Figs. 7 and 8). The digitized videomicrographs and the schematic diagram depict the continuation of the process shown in Figs. 3 and 4. The separated portion of the cytoplasmic membrane finally pinches off and forms a vesicle. The remaining cytoplasmic membrane reseals. The cytoplasmic membrane again separates from the underlying

**TABLE 1 Elastic shear modulus calculation**

| OHC | Cell length (μm) | Cell radius (μm) | Pipette radius (μm) | Stiffness parameter (dyn/cm) | Correlation coefficient | Elastic shear modulus (dyn/cm) |
|---|---|---|---|---|---|---|
| 4-19#2p | 28.8 | 5.2 | 1.8 | 0.73 | 0.994 | 14.6 |
| 4-20#1p | 44.0 | 4.6 | 1.9 | 0.92 | 0.991 | 14.8 |
| 4-19#1p | 45.2 | 4.4 | 1.8 | 1.34 | 0.991 | 19.9 |
| 3-31#1p | 57.7 | 4.1 | 1.7 | 0.65 | 0.988 | 8.8 |
| 3-31#2p | 58.1 | 4.3 | 1.7 | 0.67 | 0.985 | 9.8 |
| 3-30#1p | 68.4 | 4.0 | 1.7 | 1.21 | 0.987 | 15.7 |
| 4-7#4p | 69.3 | 4.5 | 1.5 | 1.23 | 0.994 | 20.1 |
| 4-7#7p | 71.8 | 4.3 | 1.5 | 1.06 | 1.000 | 16.1 |
| 4-7#3p | 72.1 | 4.1 | 1.5 | 1.09 | 0.992 | 15.2 |
| 4-7#5p | 72.6 | 4.2 | 1.5 | 1.23 | 0.995 | 17.8 |
| 4-7#6p | 72.8 | 4.2 | 1.5 | 1.03 | 0.999 | 14.9 |
| 4-7#2p | 73.7 | 4.1 | 1.5 | 1.31 | 0.992 | 18.2 |
| 4-7#8p | 73.7 | 3.8 | 1.6 | 1.36 | 0.995 | 16.3 |
| 4-7#1p | 74.1 | 3.6 | 1.6 | 1.20 | 1.000 | 12.9 |
| | Average | | 1.63 | 1.07 | | 15.4 |
| | Standard Deviation | | 0.14 | 0.24 | | 3.3 |

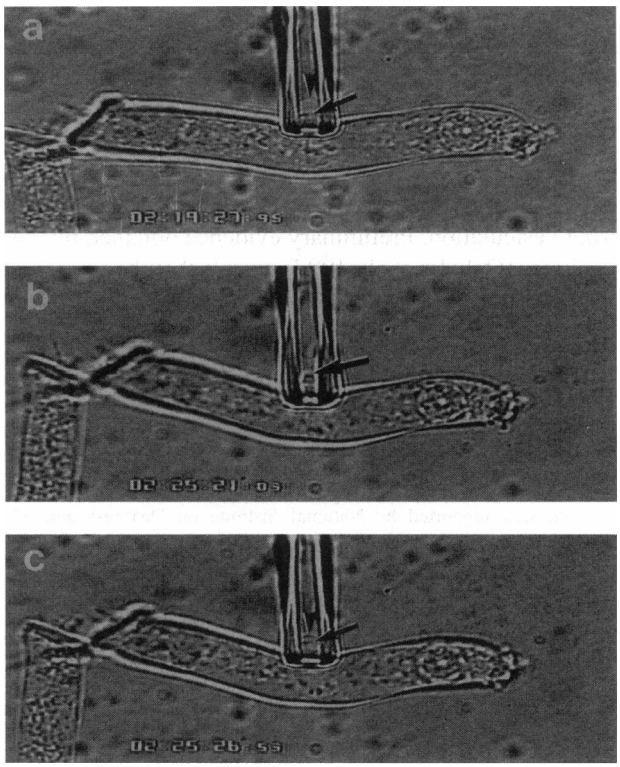


FIGURE 7 Digitized videomicrographs showing the plastic phase of the micropipette aspiration experiment (same cell as in Fig. 3). After going through the elastic phase described in Fig. 3, the cell begins to give vesicles. The pressure is kept at $-10$ cm $H_2O$ throughout the process. (*a*) Two surface layers are observed inside the micropipette. The outer one is presumed to be the cytoplasmic membrane, and the inner one the underlying structures. The bending of the cell associated with the entry of the lateral wall into the micropipette becomes conspicuous at this stage. (*b*) Formation of a vesicle. The contralateral cell wall becomes smooth and straight again. The vesicle is about 15 $\mu$m in length. (*c*) A new vesicle starts to form.

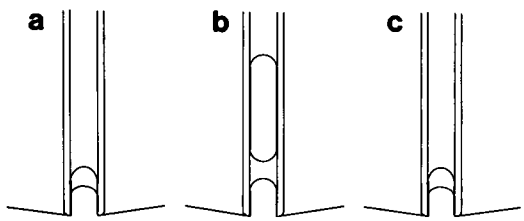


FIGURE 8 Schematic drawings corresponding to Fig. 6. (*a*) When the vesiculation pressure is reached, typically around $-10$ cm $H_2O$, the cytoplasmic membrane appears to be separated from the underlying structures and the length of the aspirated cytoplasmic membrane starts to increase. (*b*) The leading edge of the cytoplasmic membrane continues its penetration into the micropipette at the constant vesiculation pressure. The aspirated portion of the cytoplasmic membrane finally pinches off and a vesicle is formed. The cytoplasmic membrane reseals. (*c*) The vesicle moves slowly toward the widening end of the micropipette. Another portion of the cytoplasmic membrane is separated from the underlying structures. This leads to the formation of a second vesicle, and the process can be repeated many times. In some cells, a dimple can be seen on the contralateral cell wall after a few vesicles have been formed.

structures, leading to the formation of another vesicle. This process can be repeated many times. In our experiments long cells (>70 $\mu$m) release over 20 vesicles. It takes 30 s to 5 min to produce a vesicle, and vesicle size is between 10 and 20 $\mu$m. The vesiculation process reflects the mechanical properties of the cytoplasmic membrane and its interaction with the other elements of the lateral wall.

## DISCUSSION

### Lateral wall elastic moduli

Iwasa and Chadwick (1992) used a patch pipette to apply pressure pulses to OHCs and measured the resulting changes in cell radius and length. They applied linear membrane theory to analyze the data and obtained the values of shear modulus $\mu \approx 7$ dyn/cm and the ratio of $\mu$ to the area expansion modulus $\mu/K \approx 0.1$. Thus the mean value of the elastic shear modulus obtained in the present study agrees to within a factor of 2 with Iwasa and Chadwick's value. In the present study we use the value $\mu/K = 0.054$ obtained from osmotic swelling experiments on OHCs (Ratnanather et al., 1996). From this ratio and the mean value of $\mu$ obtained in the present work, we estimate the value of $K = \mu/0.054$ dyn/cm = 285 dyn/cm.

It is important to note that membrane theory, in which bending stresses are neglected, fails when it is applied to analyses of micropipette aspiration of the OHC. The reason for the failure of the membrane theory is that OHCs are long cylindrical structures, and the forces exerted by the micropipette can be viewed as a localized load. In this case, bending stresses contribute significantly to the mechanical equilibrium, thus shell theory is necessary for the analysis (Spector et al., 1996a).

The lateral wall is a composite structure, and its middle layer or cortical lattice (Bannister et al., 1988; Holley and Ashmore, 1988, 1990a; Holley et al., 1992) consists of actin filaments and spectrin cross-links (Flock et al., 1986; Holley and Ashmore, 1990b). The different properties of actin and spectrin impart anisotropy to the cortical lattice and the lateral wall. Recent data (Tolomeo and Steele, 1995; Spector et al., 1997) based on orthotropic models show that the isotropic model overestimates the wall stiffness. A composite model of the OHC lateral wall that takes into account the interactions between the major wall components is being developed (Spector et al., 1997; Tolomeo et al., 1996). Quantitative analysis of the relative displacements of the wall elements and the internal forces within the wall is based on knowing the elastic properties of such components as the plasma membrane, the cortical lattice, the subsurface cisternae, and the radial pillars, which are as yet unknown.

Micropipette aspiration technique has been applied to other cells. Table 2 presents a comparison of the stiffness parameters measured from different mammalian cell types. Red blood cell walls are composed of a cytoplasmic membrane and a "two-dimensional" cytoskeletal network mechanically associated with the membrane. Deformations of

**TABLE 2 Comparison of stiffness parameters measured from different mammalian cell types using micropipette aspiration**

| Type of cell | S (dyne/cm) | Reference |
|---|---|---|
| OHC | **1.07** | This work |
| Rat macrophage | 0.377 | Mege et al. (1987) |
| Bovine aortic endothelia cell | **0.303** | Sato et al. (1987b) |
| Lymphocyte | 0.17–0.19* | Ruef et al. (1991) |
| Monocyte | 0.11–0.12* | Ruef et al. (1991) |
| Bovine platelet | 0.099 | Smith et al. (1989) |
| Human platelet | 0.089 | Burris et al. (1986) |
| | 0.080 | Smith et al. (1989) |
| | 0.079 | Burris et al. (1987) |
| Neutrophils | 0.046–0.062* | Ruef et al. (1991) |
| | 0.019–0.024 | Evans and Kukan (1984) |
| Erythrocyte | 0.0137 | Evans (1973) |
| | 0.010 | Chien et al. (1978) |

Boldface denotes the value is measured by the authors. All others values were calculated from plots of aspiration pressure versus tongue length, except values indicated by an asterisk, for which value is calculated based on the linear portion of graphs of time-dependent tongue formation.

the wall can be accurately described by the membrane theory, with the values of the area expansion modulus $K \approx$ 450 dyn/cm and shear modulus $\mu \approx 0.004-0.009$ dyn/cm (Chien et al., 1978; Evans and Kukan, 1984). Therefore, the red blood cell shear modulus is three orders of magnitude smaller than that of the OHC. For flaccid red blood cells the stiffness parameter is expressed as $K_s = 2\mu$ (Evans and Skalak, 1980); thus the stiffness parameter varies in the range 0.008–0.018 dyn/cm. The area expansion modulus for OHCs is smaller than that for red blood cells. Endothelial cells, platelets, and leukocytes possess a three-dimensional cytoskeleton that traverses the cells. The stiffness parameter for bovine endothelial cells has been reported to be $K_s = 0.303$ dyn/cm (Sato et al., 1987a), which is approximately one-third that of the OHCs. The stiffness parameter is ~0.08 dyn/cm for human platelets, 0.1 dyn/cm for bovine platelets (Smith et al., 1989), 0.1 dyn/cm for human monocytes, 0.2 dyn/cm for lymphocytes, and 0.05 dyn/cm for neutrophils (Ruef et al., 1991). Thus there is a large variability of wall stiffness among different cells, and the OHC is the stiffest among the listed cells (judged by the values of the stiffness parameter).

## Vesiculation

The observed formation of vesicles inside the pipette suggests that either the cytoplasmic membrane possesses significant excess area (i.e., it is crenulated) or that membrane is inserted during the experiment. Electron micrographs reveal that the OHC cytoplasmic membrane is folded (Dieler et al, 1991; Ulfendahl and Slepecky, 1988). It appears that when a vesicle is being formed, the cytoplasmic membrane is separated from the cortical lattice, which remains associated with the SSC. Thus the aspiration experiments suggest that the cytoplasmic membrane can be pulled away from the underlying structures by a force corresponding to negative micropipette aspiration pressure that is greater than $-10$ cm $H_2O$. These data are important for estimating the forces between the cytoplasmic membrane and the underlying structures. Experiments (e.g., using fluorescent labeling of the different wall components; Discher et al., 1994) are required to definitively determine whether the cortical lattice remains associated with the SSC during vesiculation. Preliminary evidence obtained by these techniques (Oghalai et al., 1997) reveals that the vesicles do not result from insertion of SSC membrane into the plasma membrane.

We thank C. A. Bittner, M.D., for his participation during the early stages of the experiment and J. T. Ratnanather, D. Phil., for computational work. Assistance in image analysis by E. N. Deleu is greatly appreciated.

The work was supported by National Institute on Deafness and other Communication Disorders research grants DC00354 and DC02775.

## REFERENCES

Arima, T., A. Kuraoka, R. Toriya, Y. Shibata, and T. Uemura. 1991. Quick-freeze, deep-etch visualization of the "cytoskeleton spring" of cochlear outer hair cells. *Cell Tissue Res.* 263:91–97.

Bannister, L. H., H. C. Dodson, A. R. Astbury, and E. E. Douek. 1988. The cortical lattice: a highly ordered system of subsurface filaments in guinea pig cochlear outer hair cells. *Prog. Brain Res.* 74:213–219.

Brownell, W. E. 1990. Outer hair cell electromotility and otoacoustic emissions. *Ear Hear.* 11:82–92.

Brownell, W. E., C. R. Bader, D. Bertrand, and Y. de Ribaupierre. 1985. Evoked mechanical responses of isolated cochlear outer hair cell. *Science.* 227:194–196.

Brownell, W. E., and W. E. Shehata. 1990. The effect of cytoplasmic turgor pressure on the static and dynamic mechanical properties of outer hair cells. *In* The Mechanics and Biophysics of Hearing. P. Dallos, C. D. Geisler, J. W. Matthews, M. A. Ruggero, and C. R. Steele, editors. Springer-Verlag, New York. 52–60.

Burris, S. M., C. M. Smith, II, G. H. R. Rao, and J. G. White. 1987. Aspirin treatment reduces platelet resistance to deformation. *Arteriosclerosis.* 7:385–388.

Burris, S. M., C. M. Smith, II, D. Tukey, C. C. Clawson, and J. G. White. 1986. Micropipette aspiration of human platelet: influence of rewarming on deformability of chilled cells. *J. Lab. Clin. Med.* 107:238–243.

Calladine, C. R. 1983. Theory of Shell Structures. Cambridge University Press, Cambridge, England.

Cheng, L. Y. 1987. Deformation analyses in cell and developmental biology. Part 1: Formal methodology. Part 2: Mechanical experiments on cells. *J. Biomech. Eng.* 109:10–17, 18–24.

Chertoff, M. E., and W. E. Brownell. 1993. Characterization of outer cochlear hair cell turgor. *Am. J. Physiol.* 266:467–479.

Chien, S., K-L. P. Sung, R. Skalak, S. Usami, and A. Tozeren. 1978. Theoretical and experimental studies on viscoelastic properties of erythrocyte membrane. *Biophys. J.* 24:463–487.

Dieler, R., W. E. Shehata-Dieler, and W. E. Brownell. 1991. Concomitant salicylate-induced alterations of outer hair cell subsurface cisternae and electromotility. *J. Neurocytol.* 20:637–653.

Discher, D. E., N. Mohandas, and E. A. Evans. 1994. Molecular maps of red cell deformation: hidden elasticity and in situ connectivity. *Science.* 266:1032–1035.

Dym, C. L. 1990. Introduction to the Theory of Shells. Hemisphere Publishing Corporation, New York.

Engström, K. G., B. Moller, and H. J. Meiselman. 1992. Optical evaluation of red blood cell geometry using micropipette aspiration. *Blood Cells.* 18:241–258.

Evans, B. N. 1990. Fatal contractions: ultrastructural and electromechanical changes in outer hair cells following transmembraneous electrical stimulation. *Hear. Res.* 45:265–282.

Evans, E. A. 1973. New membrane concept applied to the analysis of fluid shear and micropipette-deformed red blood cells. *Biophys. J.* 13: 941–954.

Evans, E., and B. Kukan. 1984. Passive material behavior of granulocytes based on large deformation and recovery after deformation tests. *Blood.* 64:1028–1035.

Evans, E. A., and R. Skalak. 1980. Mechanics and Thermodynamics of Biomembranes. CRC Press, Boca Raton, FL.

Flock, Å., B. Flock, and M. Ulfendahl. 1986. Mechanisms of movement in outer hair cells and a possible structural basis. *Arch. Otorhinolaryngol.* 243:83–90.

Hochmuth, R. M. 1990. Cell biomechanics: a brief overview. *J. Biomech. Eng.* 112:233–234.

Holley, M. C., and J. F. Ashmore. 1988. A cytoskeletal spring in cochlear outer hair cells. *Nature.* 335:635–637.

Holley, M. C., and J. F. Ashmore. 1990a. A cytoskeletal spring for the control of cell shape in outer hair cells isolated from the guinea pig cochlea. *Eur. Arch. Otorhinolaryngol.* 247:4–7.

Holley, M. C., and J. F. Ashmore. 1990b. Spectrin, actin and the structure of the cortical lattice in mammalian cochlear outer hair cells. *J. Cell Sci.* 96:283–291.

Holley, M. C., F. Kalinec, and B. Kachar. 1992. Structure of the cortical cytoskeleton in mammalian outer hair cells. *J. Cell Sci.* 102:569–580.

Iwasa, K. H., and R. S. Chadwick. 1992. Elasticity and active force generation of cochlear outer hair cells. *J. Acoust. Soc. Am.* 92: 3169–3173.

Mege, J. L., C. Capo, A-M. Benoliel, and P. Bongrand. 1987. Use of cell contour analysis to evaluate the affinity between macrophage and glutaraldehyde-treated erythrocytes. *Biophys. J.* 52:177–186.

Niordsen, F. I. 1985. Shell Theory. Elsevier, Amsterdam, The Netherlands.

Novozhilov, V. V. 1959. The Theory of Thin Shells. Noordhoff, Groningen, The Netherlands.

Oghalai, J. S., A. A. Patel, T. Nakagawa, and W. E. Brownell. 1997. Visualization of OHC lateral wall composite structure under deformation. *Assoc. Res. Otolaryngol. Abs.* 20:72.

Pollice, P. A., and W. E. Brownell. 1993. Characterization of the outer hair cell's lateral wall membranes. *Hear. Res.* 70:187–196.

Ratnanather, J. T., M. Zhi, W. E. Brownell, and A. S. Popel. 1996. The ratio of elastic moduli of cochlear outer hair cells derived from osmotic experiments. *J. Acoust. Soc. Am.* 99:1025–1028.

Ruef, P., T. Böhler, and O. Linderkamp. 1991. Deformability and volume of neonatal and adult leukocytes. *Pediatr. Res.* 29:128–132.

Saito, K. 1983. Fine structure of the sensory epithelium of guinea pig organ of Corti: subsurface cisternae and lamellar bodies in the outer hair cells. *Cell Tissue Res.* 229:467–481.

Sato, M., M. J. Levesque, and R. M. Nerem. 1987a. An application of the micropipette technique to the measurement of the mechanical properties of cultured bovine endothelial cells. *J. Biomech. Eng.* 109:27–34.

Sato, M., M. J. Levesque, and R. M. Nerem. 1987b. Micropipette aspiration of cultured bovine aortic endothelial cells exposed to shear stress. *Arteriosclerosis.* 7:276–286.

Schmid-Schönbein, G. W., K-L. P. Sung, H. Tözeren, R. Skalak, and S. Chien. 1981. Passive mechanical properties of human leukocytes. *Biophys. J.* 36:243–256.

Slepecky, N., and P. J. Ligotti. 1992. Characterization of inner ear sensory hair cells after rapid freezing and freeze-substitution. *J. Neurocytol.* 21:374–381.

Smith, C. M., II, S. M. Burris, D. J. Weiss, and J. G. White. 1989. Comparison of bovine and human platelet deformability using micropipette elastimetry. *Am. J. Vet. Res.* 50:34–38.

Spector, A. A., W. E. Brownell, and A. S. Popel. 1996a. A model for cochlear outer hair cell deformations in micropipette aspiration experiments: an analytical solution. *Ann. Biomed. Eng.* 24:241–249 (see errata *Ann. Biomed. Eng.* 24(3):R6).

Spector, A. A., W. E. Brownell, and A. S. Popel. 1996b. A model of elastic properties of cell membranes. *In*: Contemporary Research in the Mechanics and Mathematics of Materials. R. C. Batra and M. F. Beatty, editors. International Center for Numerical Methods in Engineering, Barcelona, Spain. 55–66.

Spector, A. A., W. E. Brownell, and A. S. Popel. 1997. Determination of elastic moduli and bending stiffnesses of the outer hair cell wall. *Assoc. Res. Otolaryngol. Abs.* 20:72.

Theret, D. P., M. J. Levesque, M. Sato, R. M. Nerem, and L. T. Wheeler. 1988. The application of a homogeneous half-space model in the analysis of endothelial cell micropipette measurements. *J. Biomech. Eng.* 110:190–199.

Tolomeo, J. A., and C. R. Steele. 1995. Orthotropic piezoelectric properties of the cochlear outer hair cell wall. *J. Acoust. Soc. Am.* 97:3006–3011.

Tolomeo, J. A., C. R. Steele, and M. C. Holley. 1996. Mechanical properties of the lateral cortex of mammalian auditory outer hair cells. *Biophys. J.* 71:421–429.

Ulfendahl, M., and N. Slepecky. 1988. Ultrastructural correlates of inner ear sensory cell shortening. *J. Submicrosc. Cytol. Pathol.* 20:47–51.